Supporting Information

Multifunctional Iron-Carbon Nanocomposites through an Aerosol-Based Process for the *In Situ* Remediation of Chlorinated Hydrocarbons

Jingjing Zhan,[†,*] Igor Kolesnichenko,[†] Bhanukiran Sunkara,[†] Jibao He,[‡] Gary L. McPherson,[§] Gerhard Piringer,[‖] and Vijay T. John [†,*]

[†] Department of Chemical and Biomolecular Engineering, Tulane University, New Orleans LA 70118

[‡] Coordinated Instrumentation Facility, Tulane University, New Orleans LA 70118

[§] Department of Chemistry, Tulane University, New Orleans LA 70118

[‖] Department of Earth and Environmental Sciences, Tulane University, New Orleans LA 70118

* Corresponding author. Email: vj@tulane.edu. Phone: (504) 865-5883. Fax: (504) 865-6744.

Number of Pages (Including Cover): 6

Number of Figures: 2

XRD and XPS analysis

X-ray diffraction pattern of as-synthesized Fe/C is shown in Figure S1. The peak centered at 26.6 ° corresponds to the (002) graphite-like reflection of carbon and its broadening suggests the possible presence of an amorphous phase within the carbon spheres *(1)*. Peaks at the 2θ of 44.9° (110), 65° (200) and 82.3° (211) indicate the presence of zero-valent iron. In addition, the peak centered at 35.9° attributes to iron oxide (FeO) crystalline phases due to an oxidized layer. We also carried out XPS studies to verify the presence of zero-valent iron in the sample. In the experiment, the aerosol-based Fe/C sample was spread on a carbon tape. As shown in Figure S2, photoelectron peaks at 710.0 eV and 723.3 eV are related to the binding energies of Fe ($2p_{3/2}$) and Fe ($2p_{1/2}$) of iron oxide. Importantly, the shoulder at a binding energy of 706.6 eV represents the $2p_{3/2}$ peak of zero-valent iron, which is identical to those previously reported *(2)*.

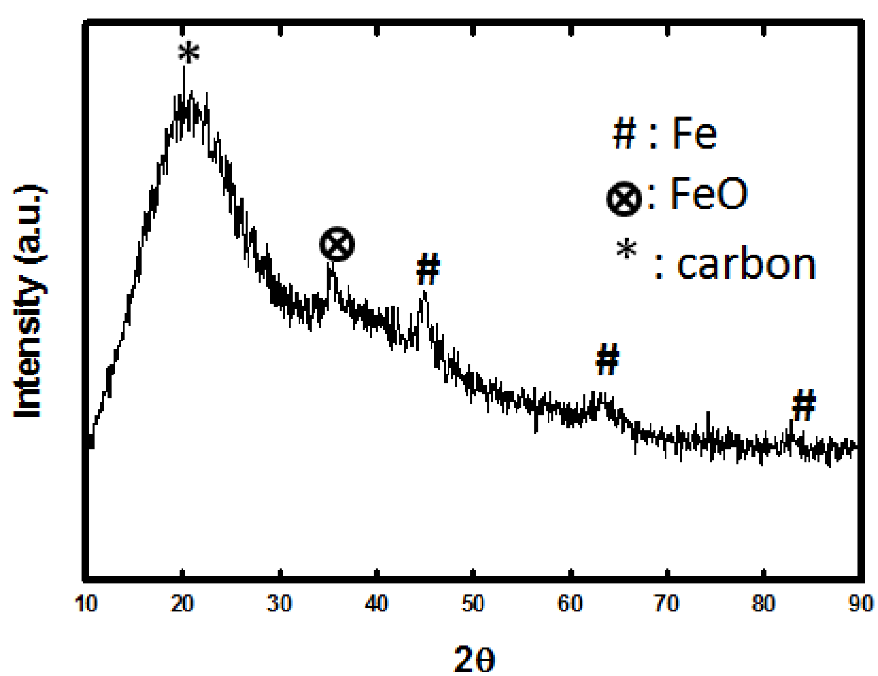

Figure S1: XRD patterns of aerosol-based Fe/ C particles.

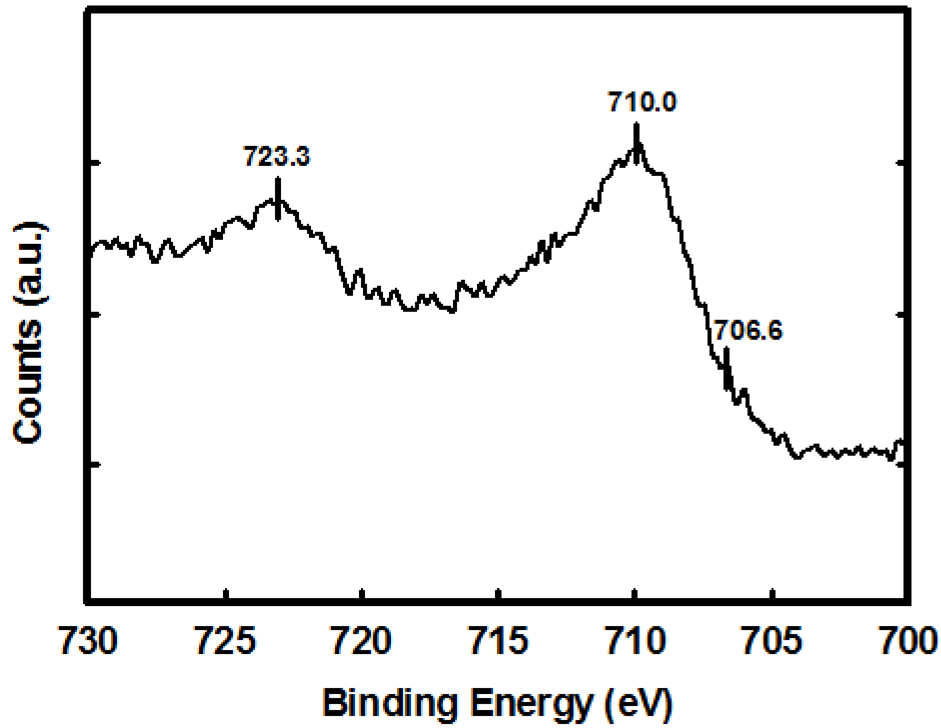

Figure S2: XPS response of Fe 2p core levels of aerosol-based Fe/ C particles.

Partitioning Characteristics

We have calculated the partition coefficient for TCE adsorption on the aerosol-based Fe/C particles using the definition of Phenrat and coworkers *(3)*:

$$\frac{C_{TCE}^{ads}}{C_{TCE}^{water}} = K_p$$

$$= \left\{ \frac{\left[\left(C_{TCE}^{Air}\right)_{ref} V_{hs} - \left(C_{TCE}^{Air}\right)_{ads} V_{hs}\right] + \left[\left(\frac{C_{TCE}^{Air}}{K_H^{TCE^*}} V_{water}\right)_{ref} - \left(\frac{C_{TCE}^{Air}}{K_H^{TCE^*}} V_{water}\right)_{ads}\right]}{\left(\frac{M_p}{\rho_p}\right)\left(\frac{C_{TCE}^{Air}}{K_H^{TCE^*}}\right)_{ads}} \right\}$$

Where C_{TCE}^{ads} is the concentration of TCE on the adsorbent (mol/L), C_{TCE}^{water} is the concentration of TCE in the water phase (mol/L), C_{TCE}^{Air} is the concentration of TCE in the headspace (mol/L), V_{hs} and V_{water} are the volumes of the headspace and water, respectively (L), M_{ads} is the mass of the adsorbent (g), ρ_{ads} is the density of the adsorbent (g/L). The subscripts *ref* and *ads* refer to the system without and with the adsorbent. $K_H^{TCE^*}$ is the Henry's law constant for TCE partitioning in water, with a value of 0.343 at 25^0C *(4)*. By this equation, the measured partition coefficient for TCE adsorption on humic acid is 85, while K_p for the adsorption of TCE on aerosol-based Fe/C composites is 1560, an 18.3 fold increase in adsorption capacity.

Calculations of sticking coefficient (α)

The sticking coefficient (α), representing the fraction of contacts between particles and collectors that result in attachment, is calculated from capillary column breakthrough data using the following equation *(5, 6)*:

$$\alpha = \frac{-2d_c ln(^C/_{C_0})}{3(1-f)\eta_0 L}$$

Where *dc*: the average diameter of sand grains;

C and C_0 are effluent and influent particle concentration;

f: the porosity of the sand grains;

L: the length of the column;

η_0: the single-collector efficiency, which can be calculated by Tufenkji-Elimelech (T-E) equation as the following *(5)*:

$$\eta_0 = 2.4A_S^{1/3}N_R^{-0.081}N_{Pe}^{-0.715}N_{vdW}^{0.052} + 0.55A_S N_R^{1.675}N_A^{0.125} + 0.22N_R^{-0.24}N_G^{1.11}N_{vdW}^{0.053}$$

We calculated the sticking coefficient based on the following conditions:

Porosity, $f = 0.32$, as measured by comparing the weight of the dry column with that of the water saturated column *(7, 8)*.

Sand size: dc = 500 μm. Ottawa sand has a board size distribution from 100 μm to 900 μm based on the observation by the optical microscopy (Olympus IX71, Japan). Here, we use the average size 500 μm in the calculation.

Absolute fluid viscosity, $\mu = 1.0*10^{-3}$ N.s/m^2

Boltzman constant, $k = 1.38065*10^{-23}$ J/K

Temperature, T = 298 K

Hamaker constant *(9)*, $H = 1.09*10^{-19}$ J

Particle size: d_p = 500 nm

Volumetric flow rate = 0.1 mL/min = $8.3*10^{-4}$ m/s

$$\text{Density of Fe/carbon particles} = \frac{\text{mass of Fe/carbon}}{\text{volume of Fe/carbon}}$$

$$= \frac{\text{mass of Fe/carbon}}{\text{volume of Fe} + \text{volumeof carbon}} = \frac{1\text{g}}{\frac{15\% * 1\text{g}}{7.8\text{g/mL}} + \frac{85\% * 1\text{g}}{2.26\text{g/mL}}}$$

$$= 2.5\text{g/mL} = 2.5 * 10^3\ \text{kg/m}^3$$

(Density of carbon particles *(10)*, ρ= 2.26 gm/mL = $2.26*10^3$ kg/m^3)

With 97% of particles eluted from the column (C/C_0=0.97) the calculated sticking coefficient is 0.09.

References:

1. Sheng, Z. M.; Wang, J. N., Thin-walled carbon nanocages: direct growth, characterization, and applications. *Adv. Mater.* **2008,** *20* (5), 1071-1075.
2. Sun, Y. P.; Li, X. Q.; Cao, J.; Zhang, W. X.; Wang, H. P., Characterization of zero-valent iron nanoparticles. *Adv. Colloid Interface Sci.* **2006,** *120*, 47.

3. Phenrat, T.; Liu, Y.; Tilton, R. D.; Lowry, G. V., Adsorbed polyelectrolyte coatings decrease Fe(0) nanoparticle reactivity with TCE in water: conceptual model and mechanisms. *Environ. Sci. Technol.* **2009,** *43* (5), 1507-1514.
4. Heron, G.; Christensen, T. H.; Enfield, C. G., Henry's Law Constant for Trichloroethylene between 10 and 95 °C. *Environ. Sci. Technol.* **1998,** *32* (10), 1433-1437.
5. Tufenkji, N.; Elimelech, M., Correlation equation for predicting single-collector efficiency in physicochemical filtration in saturated porous media. *Environ. Sci. Technol.* **2004,** *38* (2), 529.
6. Saleh, N.; Kim, H.; Phenrat, T.; Matyjaszewski, K.; Tilton, R. D.; Lowry, G. V., Ionic strength and composition affect the mobility of surface-modified Fe0 nanoparticles in water-saturated sand columns. *Environ. Sci. Technol.* **2008,** *42*, 3349.
7. Schrick, B.; Hydutsky, B. W.; Blough, J. L.; Mallouk, T. E., Delivery vehicles for zerovalent metal nanoparticles in soil and groundwater. *Chem. Mater.* **2004,** *16*, 2187.
8. Zhan, J.; Zheng, T.; Piringer, G.; Day, C.; McPherson, G. L.; Lu, Y.; Papadopoulos, K.; John, V. T., Transport Characteristics of Nanoscale Functional Zerovalent Iron/Silica Composites for in Situ Remediation of Trichloroethylene. *Environ. Sci. Technol.* **2008,** *42* (23), 8871-8876.
9. Hartley, P. A.; Parfitt, G. D., Dispersion of powders in liquids. 1. The contribution of the van der Waals force to the cohesiveness of carbon black powders. *Langmuir* **1985,** *1* (6), 651-657.
10. Ma, A.; Wang, X.; Li, T.; Liu, X.; Xu, B., Characteristics of carbon microspheres and study on its adsorption isotherms. *Mater. Sci. Eng. A* **2007,** *443*, 54-59.